Proceedings of Engineering & Technology -PET Vol 96, pp.134-141 **Advances in Energy Transition and Environmental Impacts**

ML-based bifurcation analysis of a PV pumping system

Mohamed Ali Chemkhi , Wahid Souhail, and Hedi Khammari

Laboratory of Automatic, Electrical Systems and Environment (LASEE), National Engineering School of Monastir, University of Monastir, Monastir 5019, Tunisia;

mohamedalichemkhi@gmail.com

***Abstract*— This paper introduces a novel approach utilizing machine-learning models to identify co-dimension one bifurcation points namely Limit Point (LP) and Hopf bifurcation (H) in a stand-alone PV water pumping system. With enhanced forecasting, the bifurcation diagram of the equilibrium point and trajectories are outlined more accurately. The technique determines the steady state responses and their stability. A continuation approach is used to collect training data on bifurcation structures in order to identify both stable and unstable system responses. The suggested techniques are tested using MATCONT/MATLAB, and the findings are presented.**

***Keywords*— machine learning, bifurcation; Limit point; Hopf; water pumping system**

I. INTRODUCTION

Standalone photovoltaic (PV) water pumping systems are becoming increasingly popular as a sustainable and reliable solution for water supply in remote areas, but their performance can be affected by various factors, such as changes in temperature (T) and solar irradiance (G). Understanding how these factors influence the system's behavior is crucial for ensuring optimal operation and preventing potential failures. One important aspect of understanding system behavior is analyzing the presence of bifurcations [7]. Limit point (LP) and Hopf (H) bifurcations are particularly important, potentially causing system shutdown or damaging oscillations [10]. Identifying and analyzing these bifurcations is crucial for ensuring reliable and efficient system operation. Traditionally, classical methods like mathematical modeling, stability analysis, equilibrium point analysis, and numerical continuation have been used for this purpose [2-5]. However, these methods can be computationally expensive and time-consuming, especially for complex systems. Recently, artificial intelligence (AI) techniques have emerged as promising alternatives for bifurcation analysis such as Machine learning (ML) [9] and Deep learning (Dl) [6]. AI techniques offer promising alternatives for faster and more efficient bifurcation detection. Additionally, AI-based methods can be more readily applied to real-time monitoring and control of PV water pumping systems. Among the objectives of this study, is used ML models based ANN for stand-alone PV water pumping system to detect the different bifurcation point under varying parameters, temperature, and irradiance. Firstly, we start by presents a mathematical model of a standalone photovoltaic system. That we need to study the stability of PV system. And then, a numerical study used to detect the different bifurcation points. Secondly, we suggested employing Artificial Neural Networks with basic machine-learned models and training techniques in order to design systems that are more stable, reliable and safety.

II. STAND- ALONE PV SYSTEM MODELLING

The PV system being analyzed includes a PV module, DC/AC converter, PMSM, centrifugal pump, and MPPT controller as depicted in Figure 1.

Copyright © 2026
ISSN: 1737-9334

Proceedings of Engineering & Technology -PET Vol 96, pp.134-141 **Advances in Energy Transition and Environmental Impacts**

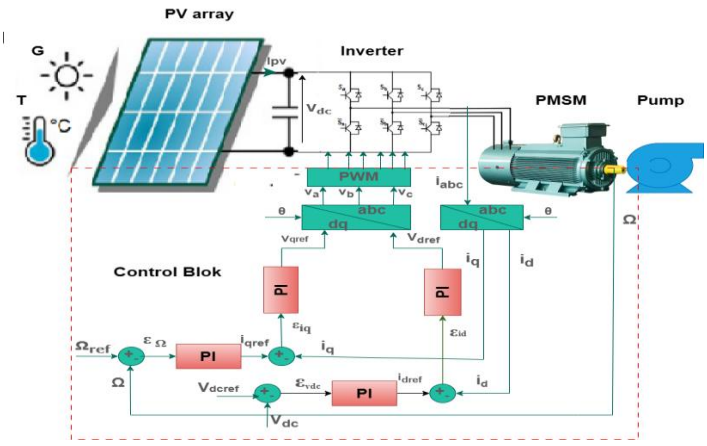

Fig1. Block diagram of the PV pumping system

A. *PV ARRAY*

The PMSM's dynamic model can be defined by three non-linear differential equations that depict the current, speed, and torque of the motor. Mathematically, the equation (1) represents the practical PV cell of single diode model

$$I_{pv} = I_L - I_0\left(\exp\left(\frac{V_{dc}+R_{spv}I_{pv}}{A}\right) - 1\right) \quad (1)$$

I_{pv} : is the solar generated current, with :

$$I_L = \frac{G}{G_{ref}}\left(I_{L,ref} + \mu_{Isc}(T_c - T_{ref})\right) \qquad I_0 = I_{0,ref}\left(\frac{T}{T_{ref}}\right)^3 \exp\left(\frac{n_s E_q}{A}\left(1 - \frac{T_{c,ref}}{T_c}\right)\right)$$

Where, I_L is the photocurrent, I_0 is the reverse saturation current of the diode.

B. *PMSM's Dynamic Model*

The PMSM's dynamic model can be defined by three non-linear differential equations that depict the current, speed, and torque of the motor [1]:

$$\begin{aligned}
\frac{di_d}{dt} &= \frac{-R_s}{L_d} i_d + \frac{pL_q}{L_d} i_q \Omega + \frac{1}{L_d} V_d \\
\frac{di_q}{dt} &= \frac{-R_s}{L_q} i_q + \frac{pL_d}{L_q} i_d \Omega - \frac{p\phi f}{L_q} \Omega + \frac{1}{L_q} V_q \\
\frac{d\Omega}{dt} &= \frac{-f}{J}\Omega + \frac{pm(L_d - L_q)}{2J} i_d i_q + \frac{pm\phi f}{2J} i_q - \frac{T_r}{J}
\end{aligned} \quad (2)$$

where i_d, i_q, and Ω are the direct-axis and quadrature-axis d–q axis currents and the angle speed respectively. The T_r is the load torque. Ld and Lq represent the inductances of the direct and quadrature-axis windings, Rs is the resistance of the stator winding, and ϕ is the magnetic flux from the permanent magnet. J represents the polar moment of inertia, the scalar f signifies the viscous damping coefficient, and p is the count of pole pairs in the motor, while m denotes the number of phases.

C. *INVERTER MODEL*

Copyright © 2026
ISSN: 1737-9334

Proceedings of Engineering & Technology -PET Vol 96, pp.134-141 **Advances in Energy Transition and Environmental Impacts**

The purpose of the inverter is to transform the direct current voltage from the PV generator into a three-phase voltage with adjustable amplitude and frequency. An inverter is driven using a natural pulse-width modulation (PWM) switching technique. The relationship given by the following equation represents the current of the capacitor.

$$c\frac{dv_{dc}}{dt} = i_{pv} - \frac{3v_d}{2v_{dc}}i_d \quad (3)$$

vd and id represent the voltage and current of the d-axis of the PMSM, respectively. The current produced by solar panels changes depending on the amount of sunlight. As a result, DC voltage may experience variations because of its nonlinear nature. The d-axis reference current generated by the DC voltage controller is determined by the voltage Vdc and control gain kpdc in equation (4) to maintain DC voltage tracking

$$i_{dref} = k_{pdc}(v_{dcref} - v_{dc}) \quad (4)$$

operates through PWM switching, where the modulation index M and the fundamental voltage Vm for the motor are provided as parameters.

$$V_m = \frac{MV}{\sqrt{2}} \quad (5)$$

III. MATHEMATICAL DESCRIPTION OF BIFURCATION THEORY

The PI regulator, a commonly used controller, can be employed for this specific purpose, with the following definition:

$$C_{PI}(t) = k_p\varepsilon(t) + k_i\int_0^t \varepsilon(t)dt \quad (6)$$

where $\varepsilon(t) = x_{ref} - x(t)$ is the error of control, x_{ref} is the reference value, and x(t) is the machine state vector. Based on this equation, the d-q reference voltages, $v = (v_{dref}, v_{qref})$, are produced by three PI controllers in the following manner:

$$v_{dref} = k_p(i_{dref} - i_d) + k_i I_{id} \quad (7)$$

$$v_{qref} = k_p(i_{qref} - i_q) + k_i I_{iq} \quad (8)$$

With:

$$I_{id} = \int_0^t (i_{dref} - i_d)dt \quad I_{iq} = \int_0^t (i_{qref} - i_q)dt$$

Using the current regulators Iid and Iiq, along with the PI regulator for angular speed, one can derive the reference current according to Equation (9).

$$i_{qref} = k_{pw}(\Omega_{ref} - \Omega) + k_{iw}\int_0^t (\Omega_{ref} - \Omega)dt \quad (9)$$

With $I_w = \int_0^t (\Omega_{ref} - \Omega)dt$

I_w is the integral speed regulator, the following differential system:

$$\frac{dI_{id}}{dt} = K_{pdc}(V_{dcref} - V_{dc}) - i_d$$

$$\frac{dI_{iq}}{dt} = -i_q - K_{pw}\Omega + K_{iw}I_w + K_{pw}\Omega_{ref} \quad (10)$$

$$\frac{dI_w}{dt} = \Omega_{dcref} - \Omega$$

Copyright © 2026
ISSN: 1737-9334

Proceedings of Engineering & Technology -PET Vol 96, pp.134-141 **Advances in Energy Transition and Environmental Impacts**

Next, the global mathematical model illustrates the behavior of a photovoltaic pumping system. A set of seven differential equations that are non-linear and one algebraic equation make up the system.

$$\frac{di_d}{dt} = -\frac{R_s}{L} i_d + p i_q \Omega + \frac{M}{\sqrt{2}L}\left(K_p\left(K_{pdc}(V_{dcref} - V_{dc}) - i_d\right) + K_i I_{id}\right)$$

$$\frac{di_q}{dt} = -\frac{R_s}{L} i_q + p i_d \Omega - \frac{p\phi}{L} + \frac{M}{\sqrt{2}L}\left(K_p\left(K_{pw}(\Omega_{dcref} - \Omega) + K_{iw} I_w - i_q\right) + K_i I_{iq}\right)$$

$$\frac{d\Omega}{dt} = -\frac{f}{J}\Omega + K_T i_q - \frac{A_p \Omega^2}{J}$$

$$\frac{dI_{id}}{dt} = K_{pdc}(V_{dcref} - V_{dc}) - i_d$$

$$\frac{dI_{iq}}{dt} = -i_q - K_{pw}\Omega + K_{iw} I_w + K_{pw}\Omega_{ref}$$

$$\frac{dI_w}{dt} = \Omega_{dcref} - \Omega$$

$$C\frac{dV_{dc}}{dt} = I_{pv} - \frac{3M}{2\sqrt{2}L}\frac{\left(K_p\left(K_{pdc}(V_{dcref} - V_{dc}) - i_d\right) + K_i I_{id}\right)}{V_{dc}}$$

$$I_{pv} = I_L - I_0\left(\exp\left(\frac{V_{dc} - R_{spv} I_{pv}}{A}\right) - 1\right) \quad (12)$$

The following equations of the form (12) are used to detect the bifurcation of the equilibrium points,

IV. The Proposed ANN Model

In the preceding section, a mathematical model was established for every subsystem, then all the submodels are combined to form the overall model for PV. In this section, first we describe the ANN approach and collect data input,output then, we training the ANN. In this study, a feed-forward neural network with supervised learning for predicting bifurcation diagrams has been used. The back-propagation learning algorithm is used for training as shown in Figure4, The inputs chosen are the temperature and irradiance levels based on weather conditions, whilst the voltage (v_{dc}), current (I_{pv}) from the PV system and Limit Point (LP), Hopf bifurcation (H) as the outputs, the hidden layer is composed of ten neurons.

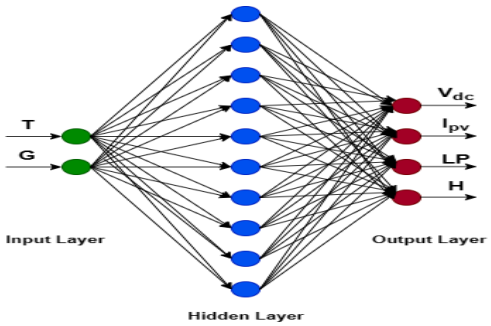

Fig2. The proposed ANN architecture

The ReLU activation function is utilized in input and hidden layers for neurons, while the output layer neurons use a linear activation function. Following the establishment of the ANN design, the data required for the training of ANN were obtained used numerical bifurcation method with system in equation (12) in Matlab/Matcont. The number of data obtained for each input and output was 23000. Those data has been divided into sub- data; 80%, 10% and 10% to train, test and validate the ANN respectively. As training algorithm, the Levenberg-Marquardt (LM) method were used. The success of the ANN was measured using mean square error (MSE)

V. Results and Discussion

Copyright © 2026
ISSN: 1737-9334

Proceedings of Engineering & Technology -PET Vol 96, pp.134-141 **Advances in Energy Transition and Environmental Impacts**

There is a different simulation scenario to detect the different bifurcation point in co-dimension one. Starting from the equilibrium point, E: x = (i_d, i_q, Ω I_{id}, I_{iq}, I_w, v_{dc}) = (-8, 17, 50, -933, 305, 1.7, 201) is represented in figure 3, where the solar irradiance constant at 100 W/m^2 and varying temperatures. The numerical bifurcation method and ANN method are agree quite well.

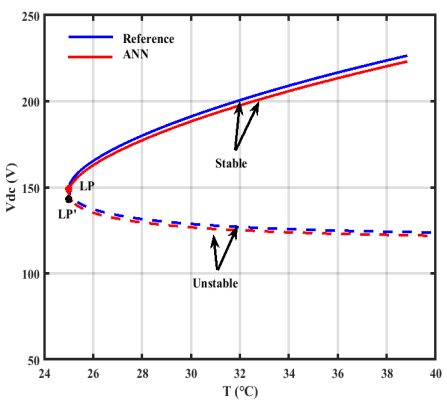

a: T-V_{dc} Bifurcation diagram

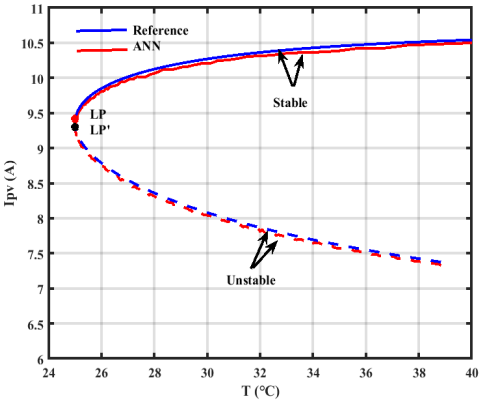

b: T-I_{pv} Bifurcation diagram

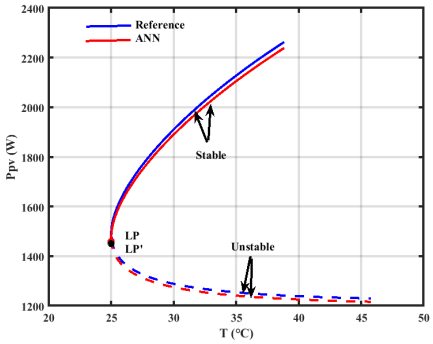

c: T-P_{pv} Bifurcation diagram

Fig3. Bifurcation diagrams

The reference LP and the predict LP' have been detected, LP x (151, 9.49, 1432), at T = 25 °C and LP' x (149, 9.47, 1411.03), at T = 25 °C. The bifurcation diagram displays the voltage, current, and power qualitative change under parameter variation. The solid blue and the red line branch represent stable parts of the curves, and the dashed blue and red line branches represent the unstable solutions. The point where the two branches intersect is referred to as the limit points LP or voltage instability point, which corresponds to the level of loading at which the two solutions combine into one solution.

Copyright © 2026
ISSN: 1737-9334

Proceedings of Engineering & Technology -PET Vol 96, pp.134-141 **Advances in Energy Transition and Environmental Impacts**

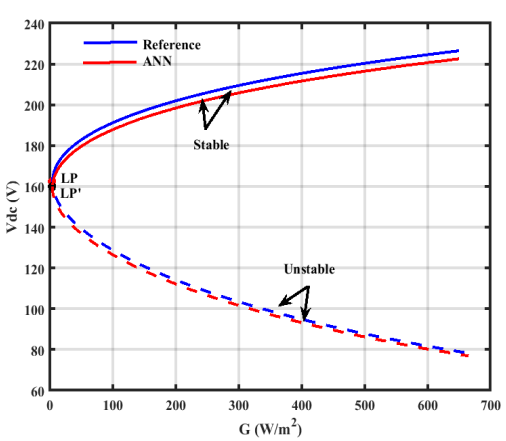

a: G-V_{dc} Bifurcation diagram

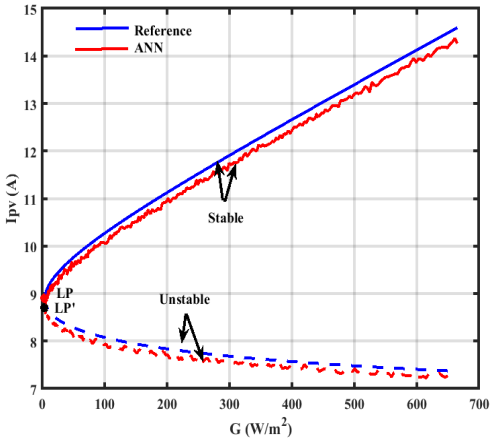

b: G-I_{pv} Bifurcation diagram

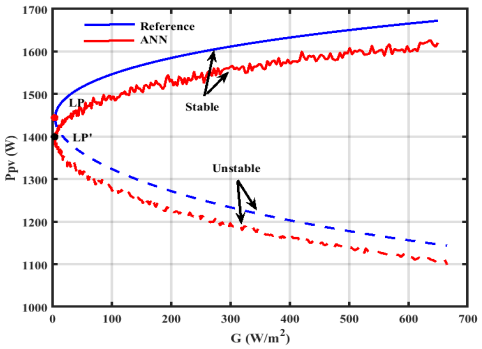

c: G-P_{pv} Bifurcation diagram

Fig4. Bifurcation diagrams

The temperature is held steady at 20°C while the bifurcation diagrams are generated by changing the irradiation, as illustrated in Figure 4. LP x (162.34, 8.9, 1444.8), at G=4.28 w/m^2 and LP' x (160.9, 8.7, 1399.8), at G=4.28 w/m^2.

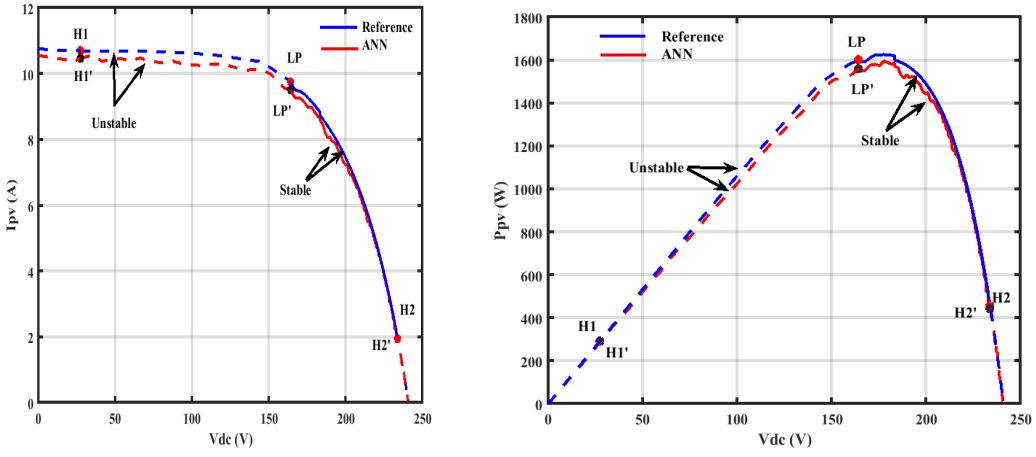

a b

Fig5. Output characteristics of the employed PV array: a I_{pv}–V_{dc} characteristics and b P_{pv}–V_{dc} characteristics

Copyright © 2026
ISSN: 1737-9334

We have examined the Ipv-Vdc and Ppv-Vdc features of a PV module at various temperature and insolation levels as shown in Figure 6, where two Hopf bifurcation points have been identified H1 x (27.46, 10.69, 293.54), H1' x (27.46,10.6, 291.07). H2 x (232.75, 2.12, 493.43), H2' x (232.75, 2, 465.5) and a limit point LPx (165.3, 9.79, 1603.4),

LP' x (165.3, 9.5, 1570.35). The bifurcation curve shows the system's operational boundaries by identifying the points that need to be avoided to prevent instability.

VI. CONCLUSIONS

Our research utilized instances of employing Artificial Neural Network technology based on machine-learning to identify various bifurcation points in stand-alone PV water pumping systems. These critical points can be identified by varying weather parameters namely the temperature, and the irradiance. This aims to ensure the PV system working within a stable range. The discussion focuses on bifurcation theory and how system parameters affect stability. By utilizing MatCont/Matlab, these methods are replicated, revealing that employing modern analysis techniques can streamline the reduction of high-dimensional equations and simplify complex calculations and transformations, ultimately making dynamic bifurcation analysis methods more practical.

REFERENCES

[1] M. A. Chemkhi, W. Souhail and H. Khammari, "ANN Based Control of MPPT in a PV System," *2023 IEEE International Conference on Artificial Intelligence & Green Energy (ICAIGE)*, Sousse, Tunisia, 2023, pp. 1-4, doi: 10.1109/ICAIGE58321.2023.10346567.

[2] J. Wu, M. Han, and M. Zhan, “Transient synchronization stability of photovoltaics integration by singular perturbation analysis,” *Front. Energy Res.*, vol. 12, no. February, pp. 1–13, 2024, doi: 10.3389/fenrg.2024.1332272.

[3] M. Abdelmoula and B. Robert, “Bifurcations and Chaos in a Photovoltaic Plant,” *International Journal of Bifurcation and Chaos*, vol. 29, no. 8. 2019. doi: 10.1142/S0218127419501025.

[4] R. He and Q. Han, “Dynamics and Stability of Permanent-Magnet Synchronous Motor,” *Mathematical Problems in Engineering*, 2017. doi: 10.1155/2017/4923987.

[5] K. Jouili and A. Madani, “Nonlinear Lyapunov Control of a Photovoltaic Water Pumping System,” *Energies*, vol. 16, no. 5, 2023, doi: 10.3390/en16052241.

[6] R. Srinivasan, “Deep neural network based MPPT algorithm and PR controller based SMO for grid connected PV system,” *Int. J. Electron.*, vol. 00, no. 00, pp. 1–20, 2021,doi:10.1080/00207217.2021.1914192.

[7] [Y. Ma, S. Lv, X. Zhou, Z. Gao, X. Zhang, and J. Zhang, “Analysis of Voltage Stability of Power Systems Using the Bifurcation Theory,” *2018 Chinese Control Decis. Conf.*, no. 50877053, pp. 5150–5155, 2018.

[8] M. A. Carbone, A. Sajadi, and S. Member, “Voltage Stability of Spacecraft Electric Power Systems for Deep Space Exploration,” *IEEE Access*, vol. 11, no. March, 2023.

[9] S. Beregi, D. A. W. Barton, D. Rezgui, and S. Neild, “Using scientific machine learning for experimental bifurcation analysis of dynamic systems,” *Mech. Syst. Signal Process.*, vol. 184, no. June 2022, doi: 10.1016/j.ymssp.2022.109649.

[10] J. Yang, C. K. Tse, and M. Huang, “Bifurcations of Grid-Following Rectifiers and Routes to Voltage Instability in Weak AC Grids,” *IEEE Trans. Power Syst.*, vol. 38, no. 2, pp. 1702–1713, 2023, doi: 10.1109/TPWRS.2022.3179287.

Copyright © 2026
ISSN: 1737-9334